All-optical fiber multi-point photoacoustic spectroscopic gas sensing system

Congzhe Zhang, [1,3,*] Yuanhong Yang, [1] Yuechuan Lin, [2,3] Yanzhen Tan, [2,3] Michael Lengden,[4] Gordon Humphries,[4] Walter Johnstone,[4] Hoi Lut Ho, [2,3] and Wei Jin[2,3]

[1]Department of Opto-electronics Engineering, School of Instrument Science & Opto-electronics Engineering, Beihang University, Beijing, China

[2]Department of Electrical Engineering, The Hong Kong Polytechnic University, Hong Kong, China

[3]Photonic Sensors Research Center, The Hong Kong Polytechnic University Shenzhen Research Institute, Shenzhen, China

[4]Centre for Microsystems & Photonics, Department of Electronic & Electrical Engineering, University of Strathclyde, 204 George Street, Glasgow, G1 1XW, UK

**Author e-mail address:czhang@buaa.edu.cn*

Abstract: An all-optical fiber multi-point photoacoustic spectroscopy gas sensing system is presented. The system can operate up to ten sensing points with a 1 ppm level C_2H_2 detection sensitivity for each sensor.

OCIS codes: (060.2370) Fiber optics sensors; (060.1155) All-optical networks; (120.5475) Pressure measurement.

1. Introduction

Photoacoustic spectroscopy (PAS) has been extensively studied for trace gas detection, as it provides a high sensitivity with a wide dynamic range, and outputs a zero-background signal [1]. Recent performance improvements in optical sources, acoustic transducers and the miniaturization of resonant acoustic cells has allowed PAS detection limits at the parts-per-million (ppm) or parts-per-billion (ppb) level to be achieved [2]. The majority of the reported PAS systems use electrical microphones as the acoustic detectors which limits remote detection and multiplexing capabilities, particularly in explosive environments. Recently, a number of all-optical fiber acoustic sensors were demonstrated [3, 4], that will allow networked remote PAS sensing. However, gas detection networks based on PAS are rarely reported.

In this paper, we report on an all-optical fiber, quasi-distributed gas detection system based on PAS technology. The system utilizes 2.5-mm-diameter multi-layer graphene diaphragm-based acoustic transducers as a replacement for standard electronic microphones. A 3x3 coupler based Sagnac interferometer is used for acoustic signal demodulation with time division multiplexing (TDM) to allow measurement of up to 10 PAS sensors. In this technique, a single pump source is used for gas excitation and PAS signal generation in up to 10 sensor heads. A single demodulation module is then used to measure the generated PAS signals using time de-multiplexing between each sensor. The system has been shown to be capable of measuring gas spectra on each of the 10 separate sensors with a detection limit of 1 ppm for C_2H_2 per sensor at 1532.8nm.

2. Experimental setup

The experimental system is shown in Fig. 1. A distributed feedback (DFB) laser with an emission wavelength of ~1532nm is used as a seed laser for an erbium doped fibre amplifier (EDFA) gas excitation 'pump' source for photoacoustic generation. To generate the photo-acoustic (PA) signals the seed laser wavelength is sinusoidally modulated in the kHz range whilst being simultaneously swept across the P(13) absorption line of acetylene at a frequency of 0.005 Hz. The modulated pump light is delivered to the 10 photoacoustic gas cells using standard SMF-28 fibre in a series fibre network, and is launched into the sensor heads and re-collected using GRIN fiber collimators. The generated acoustic signals are detected using a graphene diaphragm-based microphone similar to those described in [5]. The tip of the plug fiber on the graphene sensor is beveled at 8 degrees to avoid the reflection from the fiber end face, as shown in Fig 1 (b). The PA pressure exerted on the diaphragm during the laser gas interaction causes it to deform, and a broadband probe source (BBS) is used to measure the deformation. The resulting interferometric signal is demodulated by a 3x3 coupler based Sagnac interferometer (SI). To ensure the probe source radiation does not generate a PA signal in the gas cell a tunable filter is located at its output, which is passband tuned away from any gas absorbing wavelengths. The 3x3 coupler induces a fixed phase difference of ~120° in each output arm, which passively maintains the two outputs of the SI at quadrature when there is no acoustic induced phase difference. The two outputs are measured using a balanced detector whose output is passed to a lock-in amplifier (LIA) that demodulates the generated second-harmonic signal. A 1x16 electrically controlled optical switch (OS) is inserted into the SI to allow time-multiplexing between multiple PAS sensors using a single interferometer. In this set-up two types of gas cells were used; one 3D-printed miniature gas cell made at the University of Strathclyde [6] and the rest are non-resonant gas cells.

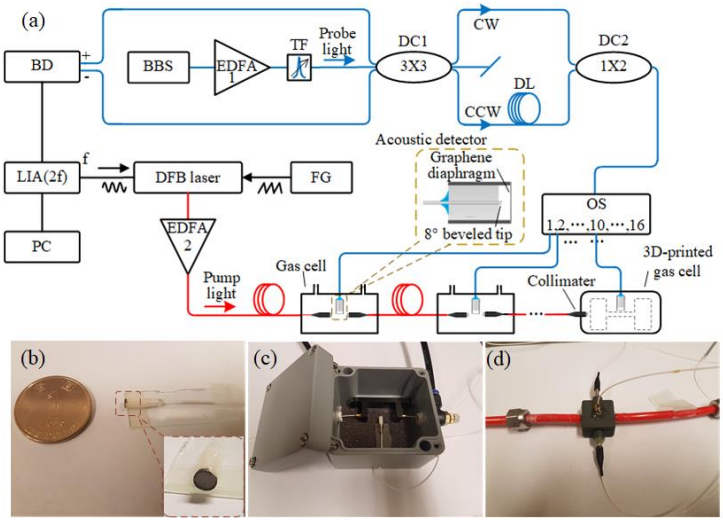

Fig. 1 Schematic of the experimental system. Blue line, Probe light, Red line, Pump light, Black line, electrical Signal, BBS, broad band source, EDFA, Erbium-doped Optical Fiber Amplifier, TF, tunable filter; DC, direct coupler; DL, delay line; LIA, lock-in amplifier; FG, function generator; DFB laser, distributed feedback laser, OS optical switch. (b) Photograph of graphene diaphragm based acoustic detector. (c) Photograph of non-resonant gas cell. (d)Photograph of 3D-printed miniature gas cell.

3. Single point measurement

Initially, the performance of the 3D-printed gas cell channel was characterized in conjunction with the graphene microphone. The 3D-printed gas cell contains a longitudinal resonator of 10 mm length and 0.9 mm radius, which leads to a theoretical resonant frequency of ~16.56 kHz. To experimentally characterize the frequency response of the system, the modulation frequency of the pump laser was varied from 6 kHz to 12 kHz at 200 Hz increments when 1000 ppm C_2H_2 balanced by nitrogen (N_2) was contained within the gas cell. The gas was flowed through the cell at a constant flow rate of 30 SCCM and the pump laser power was set to 100 mW. The second harmonic lock-in output signal, corresponding to the peak to peak output from the interferometer, is shown in Fig. 2 as a function of the modulation frequency. The maximum measured 2f signal was found to be 9.3 kHz, implying a resonant frequency is 18.6 kHz, which is significantly different to the value reported in [6]. This difference is due to the position of the front end of the microphone with respect to the pressure duct in the gas cell forming a secondary Helmholtz resonator [1]. However, this longitudinal resonance has a Q-factor of 11.5, which is similar to the Q-factor reported in [6].

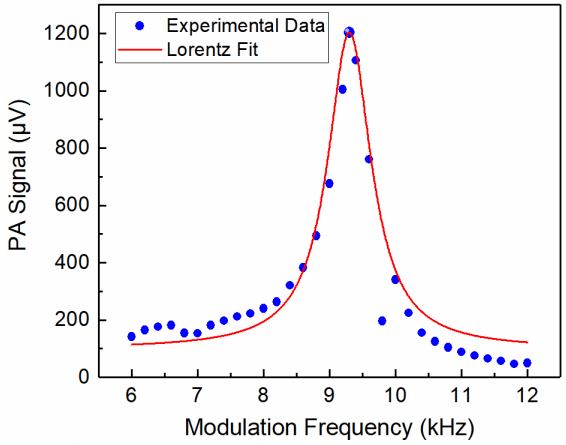

Fig. 2 Measured acoustic frequency response of the PAS sensor using second harmonic demodulation.

Fig. 3(a) shows the linear relationship between the output 2f signal and pump power, fitted by a calibration line with a linear correlation coefficient is 0.9994. In this case, the analyte gas was 100 ppm C_2H_2 balanced by N_2. The time constant of the LIA was set to 1 s with a filter slope of 18 dB Oct^{-1}. An example 2f signal is shown in Fig. 3(b) for a pump power of 140.6 mW, and has a peak-to-peak amplitude of ~169.95 μV. The system noise was obtained by measuring the standard deviation of the PA signal at a non-absorbing region, and the calculated 1σ noise level over 100 s measurement time was 0.0832 μV, giving a signal to noise (SNR) of 2042. From the SNR value, the noise equivalent concentration (NEC) is estimated to be 49 ppb, corresponding to a normalized noise equivalent absorption (NNEA) coefficient value (1σ) of 2.62×10^{-8} $cm^{-1}WHz^{-1/2}$.

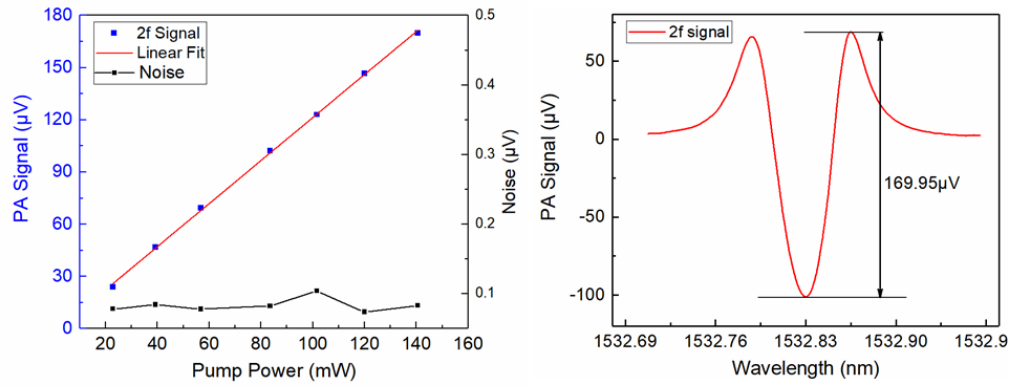

Fig. 3 (a) Peak-to-peak amplitude of second-harmonic signal and the s.d. of the noise as a function of pump power level. Blue dots: 2f signal. Red curve: Linear fit curve. Black dots: the s.d. of the noise. (b) Second harmonic LIA output when the pump wavelength is tuned across the absorption line. The pump power is ~140.6 mW.

The PA signal amplitudes of different C_2H_2 concentration level were measured within the range from 10 ppm to 200 ppm. The result is given in Fig. 4 demonstrating good linearity of the sensor as a function of C_2H_2 concentration (R^2=0.9975).

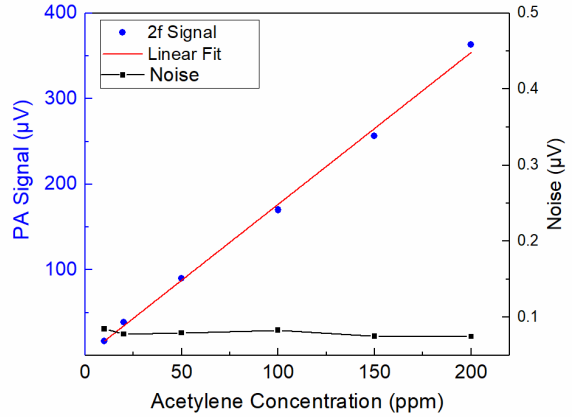

Fig. 4 Peak-to-peak amplitude of second-harmonic signal as a function of acetylene concentration level. Blue dots: 2f signal. Red curve: Linear fit curve. Black dots: the s.d. of the noise.

We also conducted Allan-Werle deviation analysis, based on the measured 2f signal recorded over a one-hour period. This provided data on the long-term stability and achievable minimum detection limit for the system. The time constant of the LIA was set to 1 s and the sampling interval time was 2 s. The resulting data are shown in Fig. 5, showing an optimum integration time of around 100 s, corresponding to a NEC of 11.8 ppb.

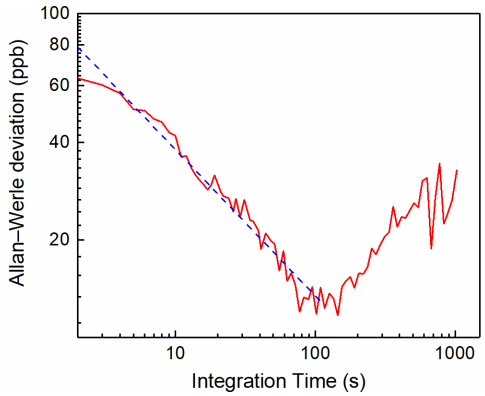

Fig. 5 Allan deviation plot for 100 ppm C_2H_2 using a 2 s time delay.

4. Multi-point measurement

To analyse the performance of the system for multi-point measurement data was recorded for three of the ten channels;1, 2 and 10. Channels 1 and 2 contained non-resonant gas cells, and the insertion loss between these two channels was ~1.1 dB, whilst the loss between channels 2 and 10 is approximately 6.5 dB. Fig. 6(a) shows

the linear increase of the 2f signal as a function of increasing pump power from EDFA2 for each channel. The 2f outputs for each of the sensors, normalized for the reflectivity of the individual graphene diaphragms is shown in Fig. 6(b). For these measurements the pump power output from EDFA2 was ~151.8 mW (details listed in Table. 1). The decrease in detection sensitivity at channel 10 is mainly due to the attenuation in pump power as light is coupled through the up-stream sensors.

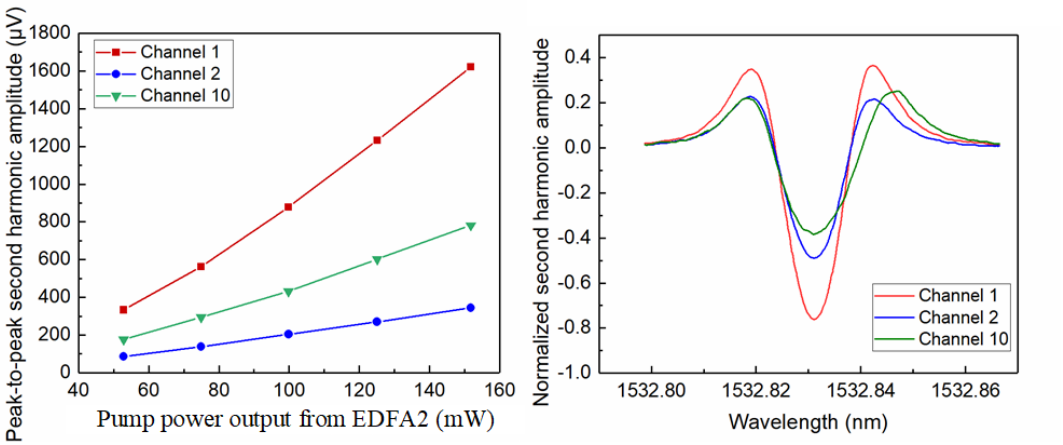

Fig. 6 (a) Peak-to-peak amplitude of second-harmonic signal and the s.d. of the noise as a function of pump power level. (b) Normalized second harmonic LIA output when the pump wavelength is tuned across the absorption. The pump power is ~140.6 mW.

Table 1 Performance of gas sensor for two different modulation frequencies

	Channel 1	Channel 2	Channel 10
Second harmonic output at absorption peak (μV)	1621.8	344.2	781.1
Noise level (μV)	0.72	0.24	0.61
SNR	2252.5	1434.1	1276.3
NEC (ppm)	0.44	0.69	0.78

5. Summary

An all-optical fiber multi-point photoacoustic spectroscopic gas sensing system has been designed and tested. For a single point measurement, a noise-equivalent PAS signal was calculated to be ~49 ppb acetylene for a 1 s data acquisition time and an optical pump power of 140.6 mW. The corresponding normalized noise equivalent absorption coefficient (NNEA) (1σ) was calculated to be 2.62×10^{-8} $cm^{-1}WHz^{-1/2}$. The system was also operated with 10 sensor heads, where the gas excitation laser was coupled in series and the acoustic detection optics were in parallel. In this case the system achieves a 1 ppm detection limit for C_2H_2 on each channel.

6. Acknowledgement

This work was supported by NSFC grants 61535004 and 61290313, and the Hong Kong Polytechnic University grants 1-ZVG4 and 4-BCD1

7. References

[1] F. Bijnen, J. Reuss, and F. Harren, "Geometrical optimization of a longitudinal resonant photoacoustic cell for sensitive and fast trace gas detection," *Review of Scientific Instruments,* vol. 67, no. 8, pp. 2914-2923, 1996.

[2] S. Borri, P. Patimisco, I. Galli, D. Mazzotti, G. Giusfredi, N. Akikusa, M. Yamanishi, G. Scamarcio, P. De Natale, and V. Spagnolo, "Intracavity quartz-enhanced photoacoustic sensor," *Applied Physics Letters,* vol. 104, no. 9, pp. -, 2014.

[3] Q. Wang, J. Wang, L. Li, and Q. Yu, "An all-optical photoacoustic spectrometer for trace gas detection," *Sensors and Actuators B: Chemical,* vol. 153, no. 1, pp. 214-218, 3/31/, 2011.

[4] Y. Tan, C. Zhang, W. Jin, F. Yang, H. L. Ho, and J. Ma, "Optical fiber photoacoustic gas sensor with graphene nano-mechanical resonator as the acoustic detector," *IEEE Journal of Selected Topics in Quantum Electronics,* vol. 23, no. 2, pp. 1-11, 2017.

[5] J. Ma, Y. Yu, and W. Jin, "Demodulation of diaphragm based acoustic sensor using Sagnac interferometer with stable phase bias," *Optics express,* vol. 23, no. 22, pp. 29268-29278, 2015.

[6] R. Bauer, G. Stewart, W. Johnstone, E. Boyd, and M. Lengden, "3D-printed miniature gas cell for photoacoustic spectroscopy of trace gases," *Opt Lett,* vol. 39, no. 16, pp. 4796-9, Aug 15, 2014.